CIGeo

Quinto Congreso en Ingeniería Geomática
Valencia, 2 – 3 de Julio de 2025
DOI: http://dx.doi.org/10.4995/CIGeo2025.2025.19873

ANALYSIS OF FIRE BEHAVIOR IN SEMI-REAL FOREST SCENARIOS BY INTEGRATING TLS DATA INTO PHYSICAL SIMULATION MODELS

ANÁLISIS DEL COMPORTAMIENTO DEL FUEGO EN ESCENARIOS FORESTALES SEMIRREALES MEDIANTE LA INTEGRACIÓN DE DATOS TLS EN MODELOS FÍSICOS DE SIMULACIÓN

Marina Simó-Martí [*], Pablo Crespo-Peremarch, Jesús Torralba, Luis Ángel Ruiz

Geo-Environmental Cartography and Remote Sensing Group (CGAT), Department of Cartographic Engineering, Geodesy and Photogrammetry, Universitat Politècnica de València, Camí de Vera s/n, 46022 València, Spain. , msimmar@upv.es; , pabcrepe@cgf.upv.es; , jetorpe@upv.es; , laruiz@upv.es

How to cite: M. Simó-Martí, P. Crespo-Peremarch, J. Torralba y L.Á. Ruiz. 2025. Analysis of fire behavior in semi-real forest scenarios by integrating TLS data into physical simulation models. En libro de actas: *Quinto Congreso en Ingeniería Geomática*. Valencia, 2 – 3 de Julio de 2025. http://dx.doi.org/10.4995/CIGeo2025.2025.19873

Abstract:

In view of the increasing intensity and frequency of large forest fires, the study and simulation of fire behavior in Mediterranean forests appears as a crucial task to define prevention and extinction strategies. The physical model Fire Dynamics Simulator (FDS) allows the analysis of fire behavior in 3D scenarios at high levels of resolution by introducing LiDAR point clouds to describe the structure and characteristics of the vegetation. The main objective of this paper is the analysis of fire behavior in Mediterranean forest semi-real scenarios, by modifying structural properties of the forest related to the horizontal and vertical continuity of the vegetation. To achieve this goal, a methodology has been developed to generate scenarios from real segmented and voxelized individuals of Mediterranean shrubland and tree species. These models were obtained from TLS (Terrestrial Laser Scanning) in plots located in *La Serra d'Espadà*. The methodology considers the distribution of biomass at individual and voxel level, taking into account a heterogeneous distribution of the bulk density of forest fuel, estimated based on the proportion of returns from the point cloud. Finally, for the analysis of the results, the evolution graphs of the following model output variables have been studied: the rate of spread, the heat release rate, the mass loss rate and the percentage of biomass consumed. Preliminary findings indicate that horizontal continuity of vegetation is the main driver for the development of steady and sustained fires.

Key words: Horizontal fuel continuity, LiDAR, Fire modelling, Bulk density, FDS

Resumen:

Ante el aumento de la intensidad y frecuencia de los grandes incendios forestales, el estudio y simulación del comportamiento del fuego en los bosques mediterráneos aparece como una tarea crucial para definir las estrategias de prevención y extinción. El modelo físico *Fire Dynamics Simulator* (FDS) permite analizar el comportamiento del fuego en escenarios 3D a altos niveles de resolución mediante la introducción de nubes de puntos LiDAR que describen de forma precisa la estructura y las características de la vegetación. El objetivo principal del presente artículo es el análisis del comportamiento del fuego en escenarios semirreales de bosque mediterráneo, modificando propiedades estructurales del bosque relacionadas con la continuidad horizontal y vertical de la vegetación. Para su consecución, se ha desarrollado una metodología que permite generar escenarios a partir de individuos reales segmentados y voxelizados de especies de matorral y árboles mediterráneos. Estos modelos se obtuvieron del escaneo TLS (*Terrestrial Laser Scanning*) de las parcelas de estudio localizadas en *La Serra d'Espadà*. La metodología contempla la distribución de la biomasa a nivel de individuo y vóxel teniendo en cuenta una distribución heterogénea de la densidad aparente (o *bulk density*) del combustible forestal, estimada en función de la proporción de retornos de la nube de puntos. Finalmente, para el análisis de los resultados se han estudiado los gráficos de evolución de las siguientes variables de salida del modelo: la velocidad de propagación del fuego, la tasa de liberación de calor, la tasa de consumo de biomasa y el porcentaje de biomasa consumida. Los resultados preliminares indican que la continuidad horizontal de la vegetación es el principal impulsor para el desarrollo y la progresión de incendios.

Palabras clave: Continuidad horizontal del combustible, LiDAR, Modelización del fuego, Densidad aparente del combustible, FDS

[*] Corresponding Author: Marina Simó-Martí, msimmar@upv.es

1. Introduction

Over the past few decades, forest fires have assumed an increasingly significant role in the Mediterranean forest landscape. What was once considered a natural ecological process has evolved into a major environmental issue. Even though the total number of wildfires in Spain has declined, large forest fires (LFF)—defined as those impacting more than 500 hectares—have become more intense, more destructive, and more frequent beyond the traditional summer season (López and López 2019). In 2022, LFFs accounted for just 0.54% of all recorded fire (MITECO 2023) yet they were responsible for burning 80.78% of the total affected area.

Several factors explain this shift in fire dynamics. Climate change has intensified the environmental conditions that trigger forest fuel ignitions, such as higher temperatures and extended droughts. Simultaneously, the accumulation and continuity of woody vegetation have grown over recent decades. We refer to fuel continuity as “the degree or extent of continuous or uninterrupted distribution of fuel particles in a fuel bed thus affecting a fire’s ability to sustain combustion and spread” (Drury 2020). This increase is largely due to forest conservation policies, rural exodus, a decline in forest resources extraction, the reduction of extensive livestock grazing, and insufficient forest management interventions (Pausas and Keeley 2021). Altogether, these factors lead to a greater build-up of combustible material in forests, resulting in larger burned areas and the release of more energy during each wildfire.

In this context, the study and simulation of fire behavior in forested areas, and especially in the forests of the Mediterranean region, appears to be a crucial task for defining forest fire prevention and suppression strategies. Currently, there is a wide variety of operational models capable of generating fire simulations that can be divided in two main groups: semi-empyrical models such as FARSITE (Finney 2006) and BehavePlus (Andrews 2014); and physics-based models such as FIRETEC (Linn *et al*. 2013) and FDS. This latter model allows for highly detailed 3D fire modelling in forest contexts (Mell *et al*. 2011) and it requires the input of three-dimensional forest structure data, which can be acquired with laser scanning remote sensing systems (LiDAR; Light Detection and Ranging).

The main objective of this paper is the modelling and analysis of fire behavior in Mediterranean forest semi-real scenarios, by modifying structural properties of the forest related to the horizontal continuity of the vegetation. To achieve this goal, a methodology has been developed to generate scenarios from real segmented and voxelized individuals of Mediterranean shrubland species.

2. Materials and Methods

2.1. Study area

The study area is located in *La Serra d’Espadà* Natural Park (Castelló, Spain) approximately at the coordinates 39.96° N and 0.41° W. The vegetation of the area is characteristic of the Mediterranean forest, with predominance of pine forests of *Pinus halepensis* Mill. and *Pinus pinaster* Aiton, occasionally accompanied by *Quercus suber* L. In our study plots there are scrub formations of *Cistus albidus* L., *Genista scorpius* (L.) DC., *Calicotome sp*., *Quercus coccifera* L., *Lavandula stoechas* L., *Daphne gnidium* L., *Ruscus aculeatus* L., *Salvia rosmarinus* Schleid. and *Pistacia lentiscus* L.

2.2. Data collection

Data collection is the first step in our designed workflow displayed in Figure 1. Surface fuel data and TLS data were acquired in our study area on different dates.

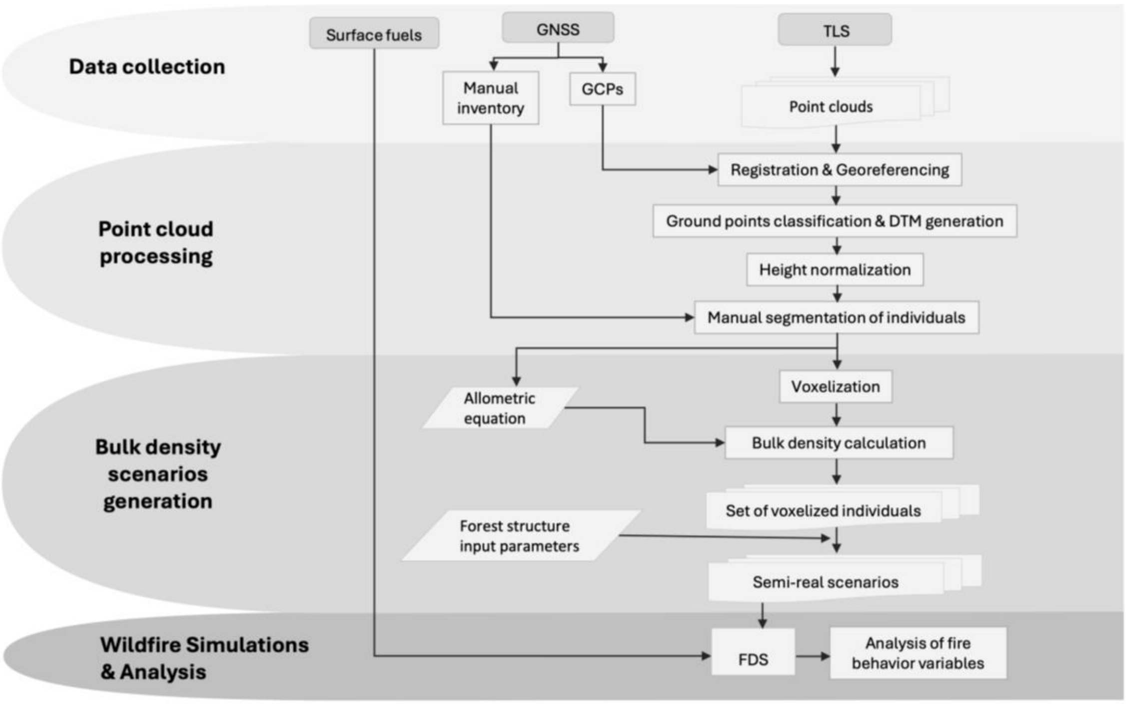

Figure 1: Methodology followed in the present work.

2.2.1. Terrestrial Laser Scanner point clouds

TLS data were recorded on May 18, 2023, using a Trimble TX6 3D laser scanner. This device emits a wavelength of 1,500 nm, an angular accuracy of 80 µrad, and a systematic range error of less than 2 mm. Five scans were taken in each plot: one central scan and four additional scans located 7.5 meters away in the cardinal directions, following the methodology proposed by Torralba *et al*. (2022). The scans were captured in maximum resolution mode with a recording time of 21 minutes. At least three spherical targets were placed in each plot and georeferenced using a Global Navigation Satellite System (GNSS) with a Leica Zeno FLX100 receiver, connected to the Valencia Reference Station Geodetic Network (ERVA) to obtain a Real-Time Kinematic (RTK) solution. This approach achieved a nominal horizontal accuracy of ± 2 cm + 1 ppm and a nominal vertical accuracy of ± 3 cm + 1 ppm. Subsequently, the TLS point clouds were registered and georeferenced using Trimble RealWorks© v12.4 software, with an average registration and georeferencing accuracy of 0.004 m and 0.284 m, respectively.

2.2.2. Surface fuel field data

For the herbaceous layer characterization (composed by *Brachypodium retusum*), 4 microplots of 0.25 m^2 and a canopy cover of 100% were randomly sampled in January 2025. On each of them the depth (cm) and the fuel load (kg·m^{-2}) were measured for further calculation of bulk density. For fuel load measurement, all the aboveground biomass of *B.retusum* was cut, dried, and weighed in the laboratory at a temperature of 105ºC for 3 hours (Shreve *et al*. 2006).

2.3. Point clouds processing

After data collection, LAStools (Isenburg 2018) was used for georeferencing TLS scans, identifying ground control points (GCPs), and creating the Digital Terrain Model (DTM) for each plot. Afterwards, the DTM was used for the normalization of the point cloud heights (Torralba *et al*. 2018). Once all the plots were normalized, individual plants (shrubs and trees) were segmented manually based on their location using CloudCompare (2024) (Stovall *et al*. 2017), obtaining a set of different models of each species as segmented point clouds.

2.4. Generation of vegetation bulk density scenarios

2.4.1. Bulk density calculation

Bulk density is a key parameter for wildfire modelling, as it describes the amount of biomass in an apparent volume, which includes empty spaces (Nunes *et al*. 2022). Therefore, bulk density at the voxel level was calculated for each segmented plant. First, the segmented point clouds were voxelized at a resolution of 0.25 m. Voxel values were calculated from the ratio between the number of returns of the voxel itself and the total number of returns of the segmented plant, resulting in values between 0 and 1. These values were used later for bulk density calculation. Second, fine fuel biomass at plant level was calculated from allometric equations by species and by plant fraction (leaves and twigs) (Eqs. 1, 2, and 3) (Sánchez-Pinillos *et al*. 2021) and the dimensions measured on the segmented point cloud.

$$B_{finefuels} = 2.031 \cdot ((0.452 \cdot h^2) \cdot h \cdot 0.723)^{0.970} \quad (1)$$

$$B_{leaves} = \frac{B_{finefuels}}{3.115} \quad (2)$$

$$B_{twigs} = B_{leaves} \cdot 2.115 \quad (3)$$

where

h = height in m

$B_{finefuels}$ = biomass of fine fuels in kg

B_{leaves} = biomass of the leaf fraction in kg

B_{ftwigs} = biomass of twig fraction in kg

For the calculation of biomass at the voxel level, the biomass at the plant level was multiplied by the value of each voxel corresponding to the proportion of returns at the plant level. With this approach, we assumed that the density of LiDAR returns would be related to the distribution of biomass in the plant, considering a heterogeneous distribution of biomass within a plant. Finally, bulk density value at the voxel level was calculated from the biomass and volume values of each voxel (*i.e.*, biomass/apparent volume occupied, kg·m^{-3}).

2.4.2. Semi-real scenarios

After having a set of different voxelized individuals from each species, we created semi-real scenarios selecting different input spatial parameters (Figure 2): regular or random distribution, number of species, density of plants, canopy height, dimensions, etc. In the present article, we present regularly distributed and monospecific scenarios of *Salvia rosmarinus* shrubland with different levels of horizontal continuity.

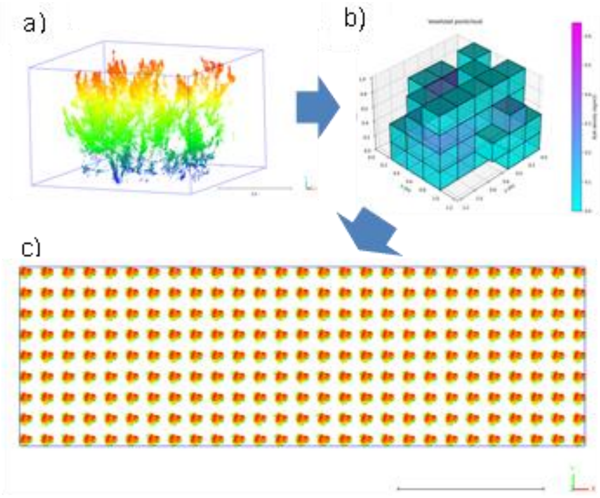

Figure 2: a) Segmented *S. rosmarinus* point cloud; b) Voxelized *S. rosmarinus* point cloud; c) Semi-real scenario of *S. rosmarinus* with 1 m gap separation between crowns.

The species *S. rosmarinus* was selected due to its high territorial representativeness in our study area and its high influence on fuel availability (Soriano and Quílez 2017). Based on their dimensions, we selected a morphologically representative individual of the *S. rosmarinus* voxelized models, and distributed it in a domain of 20 m × 60 m. By varying the gap distance between individuals (0, 0.5, 1, 1.5, and 2 m) and, in consequence, the total density of plants·m^{-2} and the percentage of canopy cover, different horizontal continuity levels of the shrub layer were achieved (Figure 2). The voxelized scenarios were converted into Fortran binary file format for FDS (McGrattan *et al.* 2023). This subsection was entirely processed with Python v.3.12.

2.5. Wildfire simulations and analysis

Wildfire simulations were executed with FDS, a Computational Fluid Dynamics Model (McGrattan *et al.* 2023) that requires the following variables to be described:

1. The dimensions of the domain and subdomains and their resolutions (Fig. 3).
2. A vegetation input file describing its bulk density distribution (see Section 2.4).
3. Fuel characteristics describing each vegetation species (bulk density, surface to volume ratio, fuel moisture, geometry and shape of leaves and branches...)
4. Other simulation parameters (wind, slope, etc.)

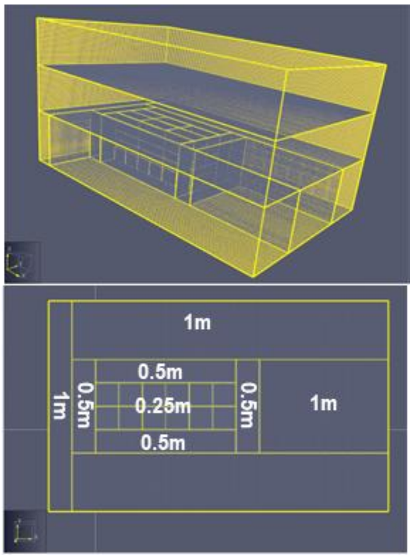

Figure 3: Domain configuration. Overview from PyroSim© 2024.2.1209 (a preprocessor for FDS). The domain was divided in several subdomains with varying resolutions to improve computational efficiency.

Tables 1 and 2 display all the common input parameters and their values (that remained constant) for our simulations. Some of the parameters were found in the literature, others were gathered from field data, and others were inferred based on our preliminary tests.

In total, 11 scenarios of dimensions 20×60 m of monospecific and regularly distributed shrubs of *S. rosmarinus* were tested varying the gap distance between shrubs (0, 0.5, 1, 1.5, and 2 m) and the presence/absence of a *B. retusum* herbaceous layer. Simulation time was set at 150 s. After completion, model outputs were obtained and Smokeview software (Forney 2025) allowed for the visualization of each simulation (Fig. 4).

Table 1: Vegetation fuel parameters.

Variables	*Value*	*Reference*
S. rosmarinus dimensions	Height = 0.824 m; Diameters = 1.274 m, 1.116 m	Field data
Herbaceous layer depth	0.21 m	Field data
Bulk density (*B. retusum*)	BD = 0.86 kg·m^{-3}	Field data
Bulk density (*S. rosmarinus*)	BD_{leaves} = 0.125 kg·m^{-3}; BD_{twigs} = 0.265 kg·m^{-3}	Calculated
Surface to volume ratio (*S. rosmarinus*)	$S{:}V_{leaves}$ = 4680 m^{-1}; $S{:}V_{twigs}$=2402.5 m^{-1}	Papió and Trabaud 1990
Surface to volume ratio (*B. retusum*)	$S{:}V_{B.\ retusum}$ = 3620 m^{-1}	Sánchez-Pinillos *et al.* 2021
Fuel moisture content	$FMC_{S.\ rosmarinus}$ = 45 %; $FMC_{B.\ retusum}$ = 20 %	Field data; Santana *et al.* 2011

Table 2: Simulation and methodological parameters.

Variable	*Value*	*Reference*
Constant wind	5.3 ms^{-1}	Based on wildfire records
Slope	0º	-
Ignition line dimensions	5×20 m	Based on our pre-test simulations
Initial HRR	534 kW	Based on our pre-test simulations
Simulation time	150 s	Based on our pre-test simulations
Time for wind development (prior to ignition)	25 s	Based on our pre-test simulations

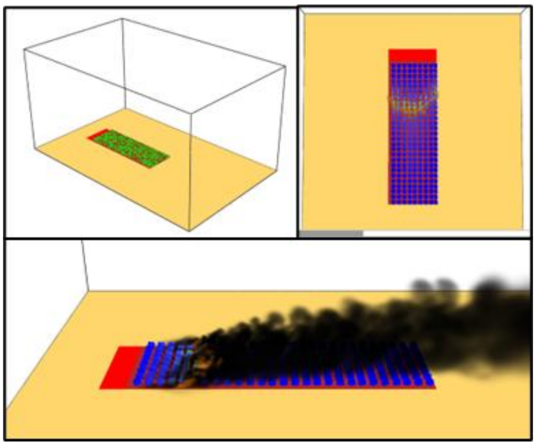

Figure 4: Visualization of one of the simulations with Smokeview, the visualization tool of FDS.

For the analysis of the results, the evolution graphs of the following model output variables were studied: the rate of spread (RoS), the heat release rate (HRR), the mass loss rate (MLR), and the percentage of total burnt dry biomass (%TBDB). The average HRR and MLR values were calculated during the steady-state phase of the fire. The average RoS value for each scenario was obtained from the RoS of three longitudinal profiles (strips 3 m wide in the x direction and 60 m long in the y direction). The position of the fire front was measured in the profiles, which were uniformly distributed to generate a representative sample and reduce the scenario edge effect. The RoS was calculated as the slope of the curve fitted to this relationship.

3. Results and discussion

Among the 11 simulations executed, 7 of them showed a sustained fire spread (we will call them "Successful" from now on) while the other 4 did not. Thus, output variables are analyzed only for the "Successful" simulations (Table 3). In particular, those scenarios composed of both a shrub layer and an herbaceous layer met the necessary conditions for fire spread, whereas scenarios lacking a continuous herbaceous layer were unable to sustain the fire. The only scenario that could hold the fire without any herbaceous layer is the one with 0 m gap distance, given that the shrub crowns were close enough to transmit the heat. As the gap distance increases, it is more difficult for the heat to be transmitted and for a sustained fire to spread. It is important to note that even though the 0-m-gap-distance scenario could sustain a fire, the HRR decreases progressively until reaching a 0 kW value (Fig. 5), which means that the *S. rosmarinus* shrub layer is not the main driver of the fire due partly to its intrinsic characteristics (bulk density, and surface to volume ratio). The *B. retusum* herbaceous layer is indeed the main layer that carries the fire spread in our simulations, which highlights the important role of continuous flammable fuel beds (Loudermilk *et al*. 2012). Higher values of HRR were obtained for the scenarios that presented a sustained fire and that had higher densities of fuel, for example, the 0-m- and the 0.5-m-gap scenarios (HRR = 163,044, HRR = 118,960 kW). In these cases, the greater accumulation of fuel and the closer distance between *S. rosmarinus* individuals allowed for a high production of energy and feedback during its thermal degradation, thus maintaining the combustion process.

Table 3: Results for sustained fire scenarios (ShL = shrub layer, HL = herbaceous layer, TBDB = total burnt dry biomass, MLR = Mass Loss Rate, HRR = Heat Release Rate, RoS = Rate of Spread, %CC = %Canopy Cover).

Gap (m)	*ShL (%CC)*	*HL (%CC)*	*TBDB (%)*	*MLR (kg·s⁻¹)*	*Mean HRR (kw)*	*RoS (m·min⁻¹)*
-	0	100	-	-	64,274	
0	82	0	60.07	3.48 /1.90	54,103	39.60
0	82	100	99.09	8.54	163,044	55.66
0.5	42	100	97.91	6.4	118,960	60.23
1	26	100	85.13	4.56	79,714	50.74
1.5	17	100	74.44	3.73	63,922	48.84
2	12	100	76.02	3.92	66,656	52.65

Regarding the proportion of biomass consumed (consumability), higher percentages of burnt dry biomass were found in denser and more continuous scenarios of shrub+herbaceous layer (0 m and 0.5 m), where all the vegetation was mostly burnt (>97%) (Table 3 and Fig. 6). An increase in discontinuity within the shrub layer was associated with a reduction in fire propagation, HRR, and overall fuel consumption. MLR values also show this evidence, and the highest values are found again in the 0 m and 0.5 m scenarios.

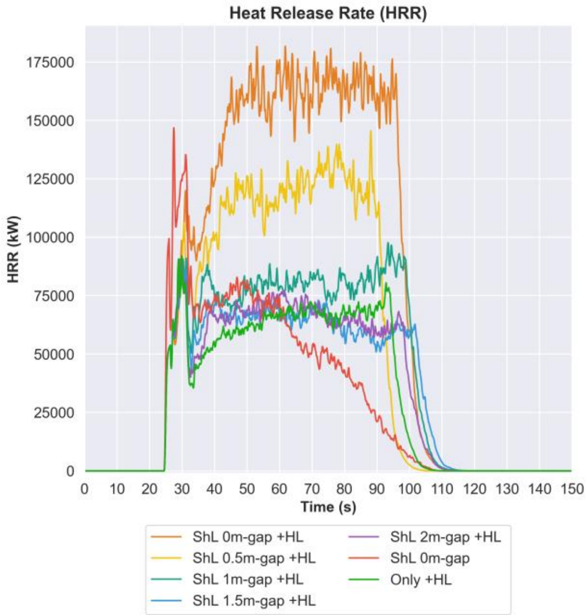

Figure 5: Evolution graph of HRR of each "Successful" scenario (ShL = shrub layer, +HL = presence of herbaceous layer).

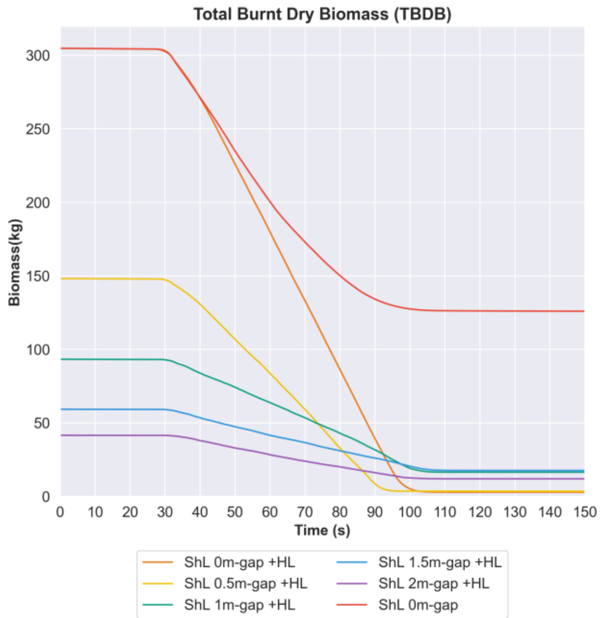

Figure 6: Evolution graph of burnt shrub biomass in each scenario with presence of shrubs (ShL = Shrub layer, +HL = presence of herbaceous layer). The graph shows how the initial amount of biomass decreases as it is consumed by the fire.

Considering the RoS, scenarios with *B. retusum* layer did not show significant differences, and a clear causal relationship cannot be inferred from the results. The highest RoS is developed in the 0.5-m-gap scenario, and the lowest in the 1.5 m gap. On one hand, it could be expected that as the canopy gap size increased, the wind flows could penetrate between the vegetation, increasing the RoS. On the other hand, scenarios with higher horizontal continuity (and fewer gaps) could also develop higher RoS due to their homogeneity in the fuel layer (Atchley *et al*. 2021). However, this behavior does not appear clear in our results. The biggest difference in RoS is found between the 0-m-gap-non-herbaceous-layer scenario and the 0-m-gap + herb-layer scenario.

4. Conclusions

After conducting the analysis and discussion of the results, the following conclusions can be drawn. First, the methodology followed allows for a good integration of TLS into wildfire simulations, thus enhancing the detail of forest structure in our semi-real scenarios. Second, fire propagation shows sensitivity to changes in the horizontal continuity of the vegetation strata (shrub and herbaceous layers), which significantly influence fire behavior, and this is clearly reflected in the simulations. In any case, a continuous fuel layer is needed for the development of a steady and sustained fire, being the herbaceous layer the main driver in our simulation study. Higher continuity results in more intense fire behavior and outreach, as it enables the combustion of a greater proportion of available biomass. Third, it is important to note that the results obtained are specific to the simulated conditions, and threshold values may vary, for example, under different wind and slope scenarios. Last, this represents the first step within a broader research work, where further inputs such as the inclusion of vertical structure and combination of all forest strata (herbaceous, shrub, and canopy) are required to support more detailed and realistic fire simulations.

Acknowledgements

We acknowledge William Mell (U.S. Forest Service) for his expert guidance and technical support during the use of the Fire Dynamics Simulator model.

This work was supported by (i) PID2020-117808RB-C21/AEI/10.13039/50110001103 and FSE+ “Invierte en tu Futuro” under Grant PRE2021-099526; and (ii) “Programa de Contratos de Acceso de Personal Investigador Doctor” (PAID-10-22) from “Vicerrectorado de Investigación de la Universitat Politècnica de València”.

References

ANDREWS, P.L., 2014. Current status and future needs of the BehavePlus Fire Modeling System. *International Journal of Wildland Fire*, **23**(1), pp. 21–33. DOI: 10.1071/WF12167

ATCHLEY, A.L., LINN, R., JONKO, A., HOFFMAN, C., HYMAN, J.D., PIMONT, F., SIEG, C., and MIDDLETON, R.S., 2021. Effects of fuel spatial distribution on wildland fire behaviour. *International Journal of Wildland Fire*, **30**(3), 179. DOI: 10.1071/WF20096

CLOUDCOMPARE, 2024. CloudCompare (version 2.13.1) [GPL software] (2.10.2 (Zephysus) Stereo). Open Source Project. Available: http://www.cloudcompare.org/ [4/20, 2025].

DRURY, S., 2020. *Fuel Continuity*. In: S. MANZELLO, ed. Encyclopedia of Wildfires and Wildland-Urban Interface (WUI) Fires. Cham: Springer International Publishing. pp. 1–3. DOI: 10.1007/978-3-319-51727-8_239-1

FINNEY, M.A., 2006. *An Overview of FlamMap Fire Modeling Capabilities*. In: P.L. ANDREWS and B.W. BUTLER, eds. Fuels Management—How to Measure Success. Portland, OR: U.S. Department of Agriculture, Forest Service, Rocky Mountain Research Station.

FORNEY, G., 2025. Smokeview, A Tool for Visualizing Fire Dynamics Simulation Data Volume I: User's Guide [online]. Gaithersburg, MD. Available: https://pages.nist.gov/fds-smv/manuals.html [6/10, 2025].

ISENBURG, M., 2018. LAStools - Efficient tools for LiDAR processing. (Version 180409). Available: http://rapidlasso.com/LAStools [4/20, 2025].

LINN, R.R., SIEG, C.H., HOFFMAN, C.M., WINTERKAMP, J.L., and MCMILLIN, J.D., 2013. Modeling wind fields and fire propagation following bark beetle outbreaks in spatially-heterogeneous pinyon-juniper woodland fuel complexes. *Agricultural and Forest Meteorology*, **173**, pp. 139–153. DOI: 10.1016/j.agrformet.2012.11.007

LÓPEZ, A. and LÓPEZ, M., 2019. Los Incendios Forestales en España. Decenio 2006-2015. [online]. Madrid. Available: https://www.miteco.gob.es/es/biodiversidad/temas/incendios-forestales/estadisticas-datos.html [12/22, 2023].

LOUDERMILK, E.L., O'BRIEN, J.J., MITCHELL, R.J., CROPPER, W.P., HIERS, J.K., GRUNWALD, S., GREGO, J., and FERNANDEZ-DIAZ, J.C., 2012. Linking complex forest fuel structure and fire behaviour at fine scales. *International Journal of Wildland Fire*, **21**(7), pp. 882–893. DOI: 10.1071/WF10116

MCGRATTAN, K., HOSTIKKA, S., FLOYD, J., MCDERMOTT, VANELL, M., and MUELLER, E., 2023. Fire Dynamics Simulator User's Guide [online]. Gaithersburg, MD. Available: https://nvlpubs.nist.gov/nistpubs/Legacy/SP/nistspecialpublication1019.pdf [12/22, 2023].

MELL, W., MCNAMARA, D., FORNEY, G.P., and HOFFMAN, C.M., 2011. Computer modelling of wildland-urban interface fires. *Fire & Materials* [online]. pp. 531–544. Available: https://www.researchgate.net/publication/267365800 [12/22, 2023].

MITECO, 2023. Los Incendios Forestales en España: 1 enero - 31 diciembre 2022 (Avance Informativo) [online]. Madrid. Available: https://www.miteco.gob.es/content/dam/miteco/es/biodiversidad/temas/incendios-forestales/Avance%20informativo%2031%20de%20diciembre%202024.pdf [02/01, 2024].

NUNES, L., PASALODOS-TATO, M., ALBERDI, I., SEQUEIRA, A.C., VEGA, J.A., SILVA, V., VIEIRA, P., and REGO, F.C., 2022. Bulk Density of Shrub Types and Tree Crowns to Use with Forest Inventories in the Iberian Peninsula. *Forests*, **13**(4). DOI: 10.3390/f13040555

PAPIÓ, C. and TRABAUD, L., 1990. Structural characteristics of fuel components of five Meditarranean shrubs. *Forest Ecology and Management*, ***35***(3-4), pp. 249-259.

PAUSAS, J.G. and KEELEY, J.E., 2021. Wildfires and global change. *Frontiers in Ecology and the Environment*, **19**(7), pp. 387–395. DOI: 10.1002/fee.2359

SÁNCHEZ-PINILLOS, M., DE CÁCERES, M., CASALS, P., ALVAREZ, A., BELTRÁN, M., PAUSAS, J.G., VAYREDA, J., and COLL, L., 2021. Spatial and temporal variations of overstory and understory fuels in Mediterranean landscapes. *Forest Ecology and Management*, **490**. DOI: 10.1016/j.foreco.2021.119094

SANTANA, V.M., BAEZA, M.J., and VALLEJO, V.R., 2011. Fuel structural traits modulating soil temperatures in different species patches of Mediterranean Basin shrublands. *International Journal of Wildland Fire*, **20**(5), pp. 668–677. DOI. 10.1071/WF10083

SHREVE, B., THIEX, N., and WOLF, M., 2006. National Forage Testing Association Reference Method: Dry Matter by Oven Drying for 3 Hours at 105º C. NFTA Reference Methods. National Forage Testing Association, Omaha, NB. Available: www.foragetesting.org [6/11, 2025].

SORIANO-SANCHO, J.L. and QUÍLEZ-MORAGA, R., 2017. Análisis de la humedad del combustible vivo en la Comunitat Valenciana. In: SOCIEDAD ESPAÑOLA DE CIENCIAS FORESTALES, ed. 7o Congreso Forestal Español. Plasencia (Cáceres, Extremadura).

STOVALL, A.E.L, VORSTER, A.G., ANDERSON, R.S., EVANGELISTA, P.H., and SHUGART, H.H., 2017. Non-destructive aboveground biomass estimation of coniferous trees using terrestrial LiDAR. *Remote Sensing of Environment*, **200**, pp. 31-42. DOI: 10.1016/j.rse.2017.08.013.

TORRALBA, J., CRESPO-PEREMARCH, P., and Ruiz, L.Á., 2018. Assessing the use of discrete, full-waveform LiDAR and TLS to classify Mediterranean forest species composition. *Revista de Teledetección*, **52**, pp. 27-40. DOI: 10.4995/raet.2018.11106.

TORRALBA, J., CARBONELL-RIVERA, J.P., RUIZ, L.Á., and CRESPO-PEREMARCH, P., 2022. Analyzing TLS Scan Distribution and Point Density for the Estimation of Forest Stand Structural Parameters. *Forests*, **13**(12), 2115. DOI: 10.3390/f13122115.